

# EMTP Tech Notes

*for users of the Electromagnetic Transients Program*

*Issue # 94-4*

*October, 1994*

*Editor: Thomas Grebe*

---

*in this issue:*

Letter from the Editor: .....	2
Digital Filtering and Relaying.....	3
Voltage Notching Concerns.....	23
Module Development Follow-up .....	33

*Letter from the Editor:*

*EMTP Tech Notes* is the technical newsletter provided to members of the EMTP User's Group. The newsletter is a quarterly technical publication highlighting contributions from members of the User's Group. This newsletter is published using Microsoft Word for Windows 6.0. If you wish to contribute an article, please contact Susie Brockman or myself for appropriate text and figure formats. Contributions in the following areas are welcome:

- Technical articles
- Modifications / enhancements to the code
- Case studies / unique simulations
- Research projects
- EMTP data preparation / model development
- Modules developed for distribution on the BBS
- Letters to the editor / User's Group
- Technical paper abstracts
- Questions for members of the User's Group

I believe that the exchange of technical information is one of the most important functions of the EMTP User's Group and this newsletter will help to serve the needs of the members. Thanks to the authors for helping to put this issue together. As always, I'm open for suggestions regarding this publication and the User's Group in general.

Thanks for your support



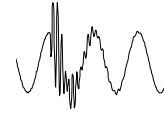
For more information concerning the newsletter or to submit a contribution please contact:

Thomas Grebe (x33) or Susie Brockman (x41)  
EMTP User's Group  
Electrotek Concepts, Inc.  
408 North Cedar Bluff Rd Suite 500  
Knoxville, Tennessee 37923  
Phone: (615) 470-9222  
FAX: (615) 470-9223

**(800) 554-4767**

# *Digital Filtering and Relaying*

---



## *Implementing Digital Filtering and Relaying in Tacs*

### *Introduction*

This discussion demonstrates the process for modeling digital relays in EMTP using TACS functions. Power system transients contain a broad frequency spectrum. Simulation of protection systems with EMTP allows one to investigate the transient response of the relay to signals at a wide band of frequencies in addition to the 60 Hz base frequency. However, conventional protection systems focus on the magnitude and phase relationships of one or more 60 Hz signals, representing power system voltages and/or currents. Relay algorithms assume that the 60 Hz signals represent some steady state or quasi-steady state conditions on the system and form the basis of trip/no-trip logic decisions. If the 60 Hz signals are steady state values, then there is no need to model using EMTP. Yet, a simple step change in the magnitude of a 60 Hz signal generates a response spread over a broad band of frequencies. This broad band of forcing functions, which can be thought of as independent sources, generated by the step change in the 60 Hz signal excites natural modes of the power network, further reinforcing the strength of these non-60 Hz signals. The natural frequencies created by resonances between capacitances and inductances of transmission lines, transformers and other power system apparatus may be close enough to the 60 Hz power signal to "confuse" the relay during the transient phase. High performance and high speed relays require that trip/no-trip decisions be made while power system transients are still a very significant portion of the measured signal. Therefore, the impact of the non-60 Hz signals on the relay response must be understood to minimize mis-operation of the relays.

The magnitude and, in most relay applications, the phase relationships of 60 Hz signals determine the vitality of the power system. The magnitude and phase of a signal are typically achieved using a time domain to phasor domain transformation algorithm. Fundamental to the success of the phasor transformation process is that the signals be at the same frequency, whether that be 60 Hz or some other frequency of interest. It would initially appear optimal to use a filter which only responds to signals very close to 60 Hz. One would soon discover that such a narrow bandwidth system would have

unacceptable slow response to changes in magnitude. Hence, the benefits of a narrow bandwidth to eliminate interference from harmonics and other sources of noise must be weighed against the time response of wide bandwidth filters.

Both electro-mechanical relays and early solid-state relays achieved the filtering functions described above using analog filters. These analog filters are constructed from a network of resistors, capacitors, and inductors in electro-mechanical relays; or from operational amplifiers in solid-state relays. Digital filters, using sampled signal levels, have been used to perform the isolation and transformation operations in more recent relays. Digital filters provide the advantages of precision, time invariance, flexibility, size, and cost to offset the disadvantages of additional analog to digital conversion complexity and finite bandwidth related to sampling rate.

### ***EMTP Implementation Issues***

Digital computers are not able to solve continuous time differential equations directly since they can only solve equations at discrete instants in time. Instead EMTP solve continuous time differential equations by using a digital approximation. EMTP bases this approximation on a trapezoidal integration scheme while some other digital simulation packages may use higher order numerical integration techniques.

The modeling of relays employing analog filters to perform 60 Hz filtering and phasor transformation using TACS requires using Laplace domain transfer functions to represent the analog networks. In the case of solid-state and electro-mechanical relays obtaining a transfer function may prove difficult due to the proprietary nature of existing documentation.

To model digital relays with TACS, one can take advantage of the transport delay function embedded within TACS to generate the time delay operations represented by  $z^{-n}$  operator in discrete time domain filters. The following discussion investigates issues associated with the bandwidth of digital filters. Two methods will be presented for the transformation of phase and magnitude based upon orthogonal basis functions. A simple time over-current relay model is developed using a TACS implementation of digital filters combining both frequency selectivity and phasor transformation operations. The sample relay model presented in this discussion is not intended to represent the digital relays of any specific manufacturer.

## Digital Filtering

A digital filter belongs to the general class of digital signal processing (DSP) algorithms that operate on a data sequence which is discrete in time and magnitude. The purpose of a digital filter is usually to separate sinusoidal signals on the basis of frequency, although, as will be demonstrated shortly, not all are restricted to frequency discrimination. The discrete time and magnitude sequence is generated by sampling an analog signal which is continuous in both time and magnitude. Results of digital filters are constrained by the Nyquist criteria which states that aliasing will occur unless the sampled continuous signal has no frequency components higher than one half the sampling rate. In general, linear digital filters are described by a ratio of two polynomials to form a discrete transfer function,  $H(z)$ , which relates discrete input sequences,  $X(z)$ , to discrete output sequences  $Y(z)$  as described by (1).

$$H(z) = \frac{Y(z)}{X(z)} = \frac{b_0 + b_1 z^{-1} + b_2 z^{-2} + \dots + b_M z^{-M}}{a_0 + a_1 z^{-1} + a_2 z^{-2} + \dots + a_N z^{-N}} \quad (1)$$

In the most general sense, the  $z^{-n}$  operator in (1) can be viewed as a transport delay function of  $n$  samples. Equation (1) can be written in the form of a difference equation expressed by (4) where there is a one to one correspondence of coefficients  $a_j$  and  $b_j$  in (1) and (4). The conversion from transfer function form, (1), to difference equation form, (4), goes as follows:

1. Express (1) as  $Y(z) D(z) = X(z) N(z)$ , where  $D(z)$  is the denominator polynomial on the right side of (1) and  $N(z)$  is the numerator polynomial on the right side of (1) as expressed in (2).

$$Y(z) a_0 + Y(z) a_1 z^{-1} + Y(z) a_2 z^{-2} + \dots + Y(z) a_N z^{-N} = X(z) b_0 + X(z) b_1 z^{-1} + X(z) b_2 z^{-2} + \dots + X(z) b_M z^{-M} \quad (2)$$

2. Since  $z^{-1}$  is used as the delay operator equal to the sample interval,  $T$ , replace every  $Y(z) z^{-i}$  by  $Y_{n-i}$  and every  $X(z) z^{-i}$  by  $X_{n-i}$  as shown in (3).

$$y_n a_0 + y_{n-1} a_1 + y_{n-2} a_2 + \dots + y_{n-N} a_N = x_n b_0 + x_{n-1} b_1 + x_{n-2} b_2 + \dots + x_{n-M} b_M \quad (3)$$

The subscripts on  $X_{n-i}$  and  $Y_{n-i}$  are shorthand notation representing the discrete time series  $Y(t = (n-i)T)$  and  $X(t = (n-i)T)$ .

3. Upon rearranging, the only unknown in equation (3) is on the left hand side of equation (4). Recognize that  $X_n$  is the most recent sampled input data value whereas all of the  $X_{n-i}$  are past samples of the input signal. Likewise,  $X_{n-i}$  and  $Y_{n-i}$  are past inputs and solutions to the difference equation.

Initially, these values are arbitrarily assigned.  $Y_n$  is the newest solution of the difference equation and is the present value of the filtered input.

$$y_n = (x_n b_0 + x_{n-1} b_1 + x_{n-2} b_2 + \dots + x_{n-M} b_M - y_{n-1} a_1 - y_{n-2} a_2 - \dots - y_{n-N} a_N) / a_0 \quad (4)$$

In general, a digital filter is the summation of weighted inputs, present and past, added to the summation of weighted past outputs as expressed by equation (5). Usually all coefficients are normalized by  $a_0$  to eliminate the need for performing a division in (4) and (5).

$$y_n = \frac{\sum_{i=0}^M b_i x_{n-i} - \sum_{i=1}^N a_i y_{n-i}}{a_0} \quad (5)$$

### ***Digital Filtering in Relaying***

Digital filtering requires processing a discrete time sequence of data as might be produced by sampling a continuous voltage or current signal using a digital to analog converter or as could be produced as an output from a time domain computer simulation, such as EMTP. This process may be used to compute the magnitude and phase of a signal within a selected band of frequencies. Extracting magnitude and phase information from a complex signal can be accomplished using a particular set of digital filters that form an orthogonal basis set, such as discrete fourier transforms (DFT) or Walsh functions.

Frequently the terms FFT (fast fourier transform) and DFT are used interchangeably. Fast fourier transforms are a specific class of DFT algorithms which require minimal computational time and effort. During this discussion FFT algorithms are included when the term DFT is used.

Walsh functions and DFT's belong to a class of filters known as FIR or finite impulse response filters. With the transform function in the form of (6) and difference equation in the form of (7), FIR filters are all zero filters (without poles) and are therefore unconditionally stable. Equations (6) and (7) correspond to (1) and (4) directly when the polynomial in the denominator is equal to a constant.

$$H(z) = \frac{Y(z)}{X(z)} = b_0 + b_1 z^{-1} + b_2 z^{-2} + \dots + b_M z^{-M} \quad (6)$$

$$y_n = x_n b_0 + x_{n-1} b_1 + x_{n-2} b_2 + \dots + x_{n-M} b_M \quad (7)$$

The solution of the difference equation in (7) follows exactly the same procedure as described for (4) above. The question now arises as to how to select the coefficients  $b_0$  through  $b_M$  to generate a set of difference equations which form an orthogonal basis set. Two different types of filters will be examined in the discussion that follows: Discrete Fourier Transform filters and Walsh functions.

Two issues must be considered when using DSP technology to determine the magnitude and phase of a signal. Caution must be exercised when processing a complex signal, i.e. a signal that is not a single frequency sinusoid. Such a signal has energy spread over a broad frequency spectrum and a time varying energy spectral distribution. Digital filters have finite bandwidth as illustrated in Figure 1. The output from the digital filters can be affected signals outside the frequency of primary interest.

The second issue deals with taking the DFT of a finite data sequence. When a sequence of discrete time values of length  $N$  are processed with a DFT or Walsh function algorithm, it is assumed that the sequence is periodic every  $N$  samples. Errors are minimized when the data sequences are changing slowly during transient periods. In the limit, errors tend toward zero only as the sequence length tends toward infinity since transients are not periodic. This reinforces the idea that the longer one has to observe the signal, the more secure the decisions which are based upon those observations will be. Digital filters with a small observation window permit faster decisions but are subject to greater transient errors.

### **DFT Filters**

Discrete Fourier Transforms apply Fourier analysis to describe a discrete time signal with the sum of sinusoidal signals applied at discrete frequencies and added through superposition. Therefore, the input to a DFT is a discrete time series of values, and the output is a discrete number of sine functions. Two FIR difference equations, in the form of (8) and (9) and with coefficients defined by (10) and (11), are required to determine each set of orthogonal values for each of the  $N/2$  bands of frequencies with index  $n$ . The nomenclature *Re* for real part and *Im* for imaginary part are used for convenience only.

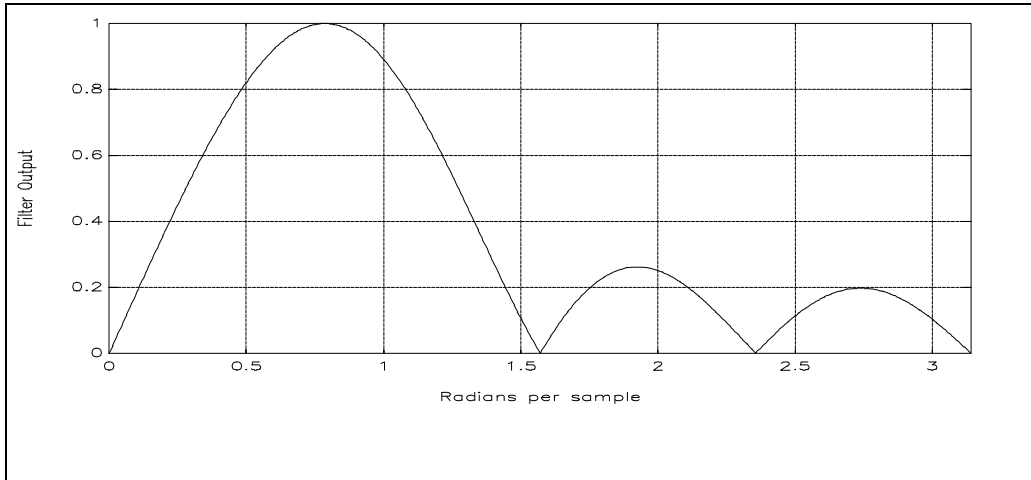


Figure 1 - Frequency Response for an 8 Point DFT with Index of 1

$$Y_{re_{jn}} = \sum_{j=0}^{N-1} A_{jk} x_{n-i} \quad (8)$$

$$Y_{im_{jn}} = \sum_{j=0}^{N-1} B_{jk} x_{n-i} \quad (9)$$

$$A_{jk} = \cos\left(\frac{2\mathbf{p}jk}{N}\right) \quad (10)$$

$$B_{jk} = \sin\left(\frac{2\mathbf{p}jk}{N}\right) \quad (11)$$

Hence,  $Y_{re_{k1}}$  and  $Y_{im_{k1}}$  for the first index represents the real and imaginary components of a single sinusoidal signal at frequency  $(2/Ts)/N$  or  $F_s/n$  where  $N$  is the number of samples,  $T_s$  is the sampling interval and  $F_s$  is the sampling rate. Any signal or signals at frequencies within a particular bandpass will be represented by a single frequency, as described by (12) for that band.

$$S_{kn} = \frac{2\sqrt{Y_{re_{kn}}^2 + Y_{im_{kn}}^2}}{N\sqrt{2}} \cos\left(2\mathbf{p}F_s \frac{k}{N} t + \tan^{-1}\left(\frac{Y_{im_{kn}}}{Y_{re_{kn}}}\right)\right) \quad (12)$$

Figure 2 shows the frequency response for the four frequency bandpass functions of an 8 point DFT. As can be seen, the bandpass filters are not ideal and have significant side lobes outside the bandpass frequencies. We can take advantage of the characteristic that a particular bandpass filter has zeros of transmission where other bandpass filters have maximum response. This is particularly attractive when the input analog signal is sampled synchronously to the frequency of the signal of primary interest. The result is that harmonics of the signal of interest are effectively suppressed. For example, if a discrete time sequence results from sampling a signal at a 480 Hz rate, the frequency response as shown in Figure 1 will have maximum response at 60 Hz. However,

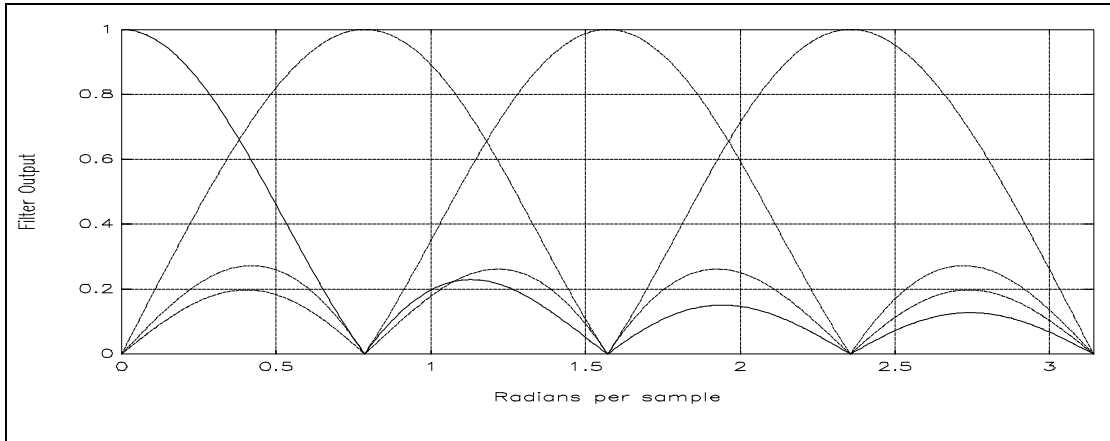


Figure 2 - Frequency Response for an 8 Point DFT for Index 0, 1, 2 and 3

as previously discussed, signals at frequencies other than the fundamental and harmonics are present due to natural modes of the network. Signal at non-harmonic frequencies can cause erroneous results from the digital filter.

The previous constraints notwithstanding, we can proceed to determine the RMS magnitude and phase of a discrete time sequence by creating two DFT filters using (8) through (11) and the magnitude scale factor from (12). Consider the example of  $N=8$ , when a discrete time data sequence is generated by sampling a continuous signal 480 times per second. The bandpass filter described by  $n=1$  will have maximum response at 60 Hz. The magnitude scale factor for this example will be  $1/(4\sqrt{2})$  and the filter coefficients as listed in Table 1.

Table 1 - Filter Coefficients for an 8 Point DFT Filter

Filter Coefficients for $Y_{re1}$		Filter Coefficients for $Y_{im1}$	
a0	1	b0	0
a1	$1/\sqrt{2}$	b1	$1/\sqrt{2}$
a3	0	b2	1
a4	$-1/\sqrt{2}$	b3	$1/\sqrt{2}$
a5	-1	b4	0
a6	$-1/\sqrt{2}$	b5	$-1/\sqrt{2}$
a7	0	b6	-1
a8	$1/\sqrt{2}$	b7	$-1/\sqrt{2}$

## Walsh Functions

Walsh functions are another form of orthogonal decomposition digital filters commonly used in RMS detectors. Like DFT RMS detectors, implementation of Walsh functions requires two equations to determine the real and imaginary parts. They have the advantage of having filter coefficients which are either unity or zero thus eliminating the need for floating point or mathematics. The coefficients for four-point Walsh functions are expressed by (13) and (14) and the conversion to RMS magnitude and phase is shown by equations (15) and (16). As with the DFT filters, an implicit assumption is a sampling rate which is synchronized with the frequency of the signal to be converted to phasor form. Figure 3 shows the TACS implementation of equations (13)-(16).

$$CAL_n = x_n - x_{n-1} - x_{n-2} + x_{n-3} \quad (13)$$

$$SAL_n = x_n + x_{n-1} - x_{n-2} - x_{n-3} \quad (14)$$

$$RMS_n = \frac{\sqrt{CAL_n^2 + SAL_n^2}}{4} \quad (15)$$

$$q_n = \tan^{-1}\left(\frac{SAL_n}{CAL_n}\right) \quad (16)$$

A simple example of implementing a digital filter in TACS is to compute the RMS current magnitude and phase from information measured in a simple power system. The RMS current calculation shows only the 60 Hz part of the signal, none of the dc offset or higher frequency noise is included. The outputs of this filter could then be sent to a digital relay or control circuit. The digital filter samples the current measured from the system four times per cycle, using the TACS sample and hold function. In this case the simulation time step is set at one fiftieth of this time period, with rounding taken into consideration. This timestep is also acceptable with the travel times for the transmission lines in the simple system.

The sampled output then goes to the delay functions, so that the sampled outputs are delayed by 1/4, 1/2, and 3/4 of a 60 Hz cycle respectively as required by (8) and (9) or (13) and (14). Synchronizing the time delays is easy, since they are equal to 1, 2, and 3 times the sample period in this case. For example, for a delay of 1/240 seconds would require that the timestep be a multiple of 1/240 seconds. Any rounding must be done carefully to preserve the proper ratio with the time step.

```

TACS HYBRID
C OUTPUT <-----A-----B-----C-----> <--T-START--<--T-STOP--
91BKRWA          60.
C
C Sample generator for 240ms sampling A to D converter
C Variable|Amplitude| Period |Time high
C OUTPUT <-----A-----B-----C-----> <--T-START--<--T-STOP--
23SAMPL          1.1   .00415   .00003
C Generate AD converter samples at 240 ms intervals
C OUTPUT <-----A-----B-----C-----> <--T-START--<--T-STOP--
88WADZ0 62+BKRWA          SAMPL
C ////////////////////////////////////////////////////////////////////
C          DIGITAL CALCULATIONS
C
C
C SAMPLE AND HOLD delayed samples
C OUTPUTvv+IN1--> +IN2--> +IN3--> +IN4--> +IN5--> <--A--<--B--<--C--<--D--<--E--
88WADZ1 53+WADZ0          .00415
88WADZ2 53+WADZ0          .00830
88WADZ3 53+WADZ0          .01245
C
C ..... WALSH FUNCTION CALCULATIONS .....
C OUTPUT +IN1--> +IN2--> +IN3--> +IN4--> +IN5--> <--gain<--low<--highLOW-->HIGH-->
WZSAL +WADZ0 +WADZ1 -WADZ2 -WADZ3          1.
WZCAL +WADZ0 -WADZ1 -WADZ2 +WADZ3          1.
88WZPHS =ATAN(WZSAL/WZCAL)*3960/7
88WZRMS =SQRT(WZSAL*WZSAL+WZCAL*WZCAL)/4
C ////////////////////////////////////////////////////////////////////

```

Figure 3 - TACS Implementation of Walsh Function.

These delayed functions are then summed with the original output to form two special DFT algorithms called Walsh functions to generate the Cal and Sal. These functions are then used to compute the RMS value and the phase as described in (13) through (16). Figure 3 the coding of this implementation in TACS.

Synchronization of the delays with the timestep is necessary to prevent gaps and/or overlaps between the signals when they are added to form the variables Cal and Sal. The effect of the error if they are not synchronized is more obvious when the RMS value is calculated from (15). Figure 4 shows the measured instantaneous current. Figures 5 and 6 show the RMS values with and without synchronization with the timestep. Note the spikes in Figure 6 due to the overlap in delay functions.

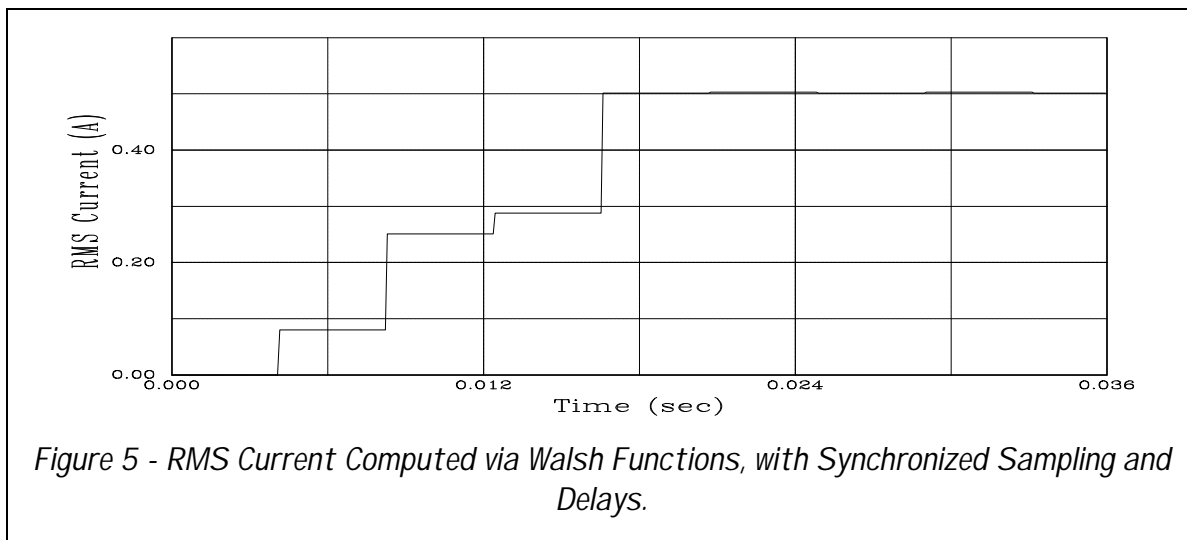
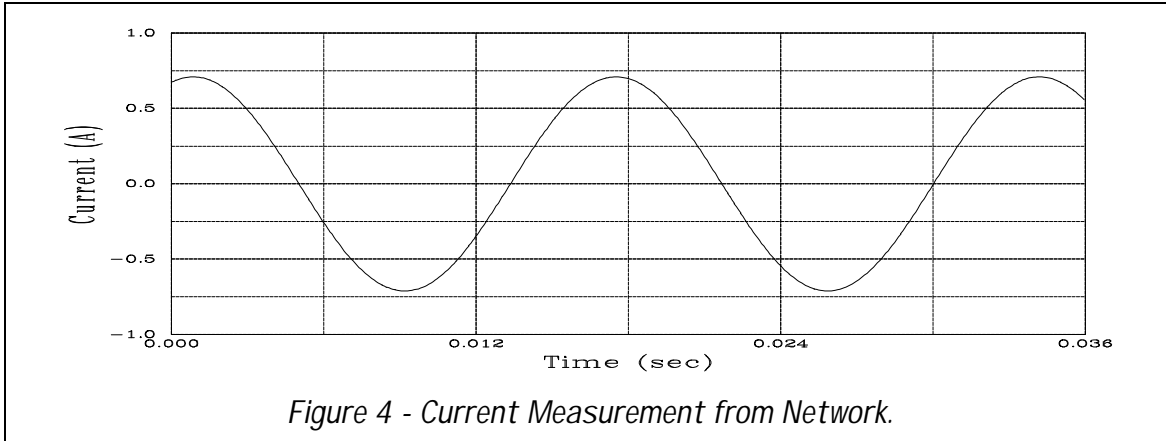
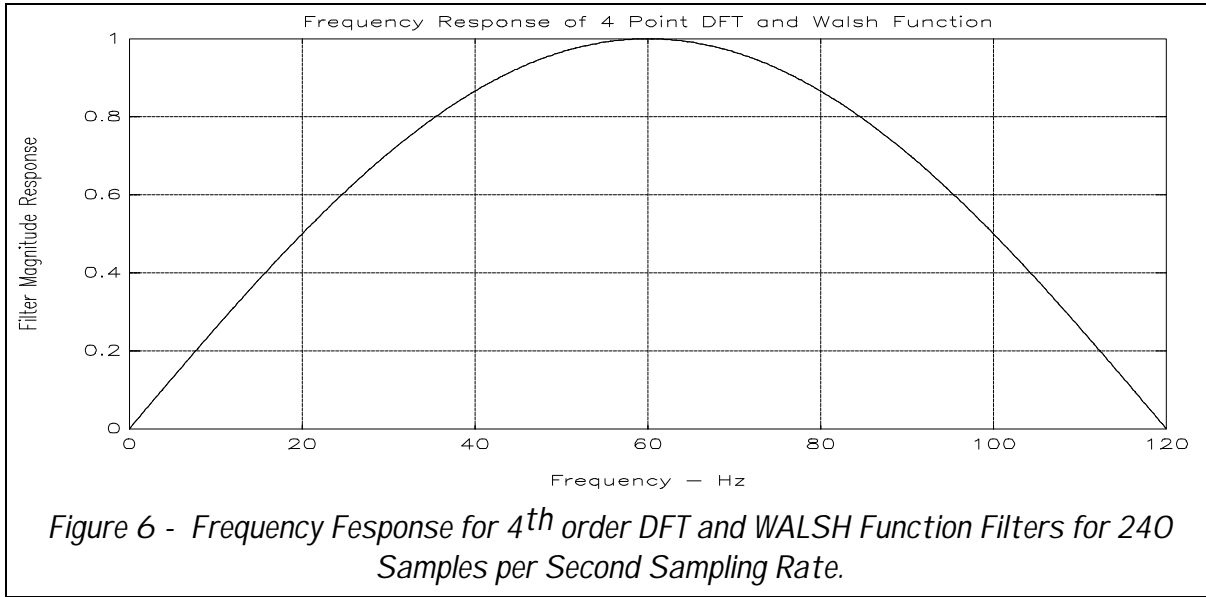


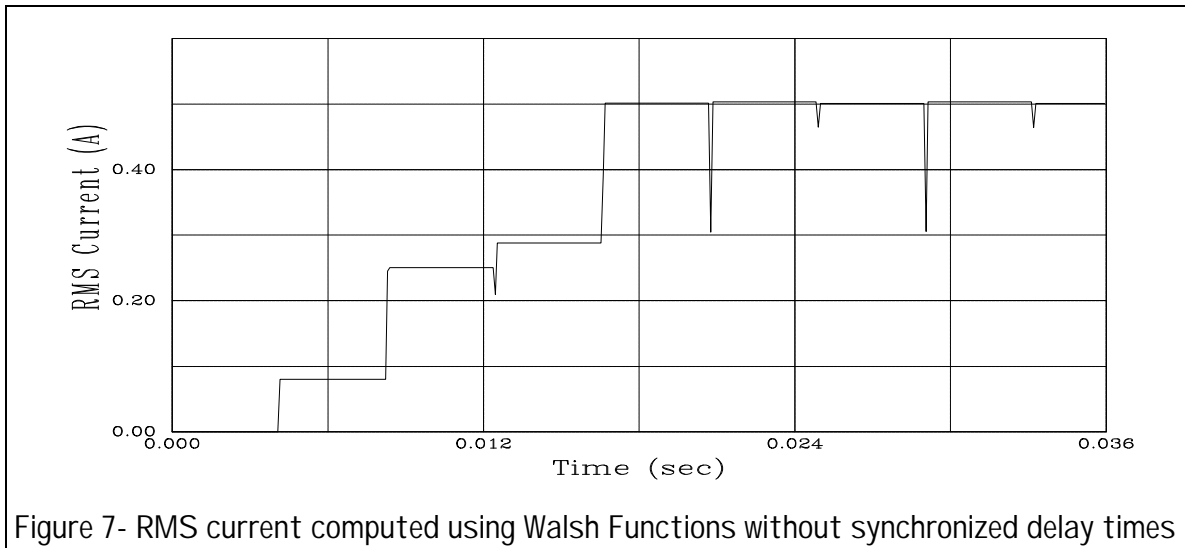
Figure 7 demonstrates that the phase results based on (12) and (16) for the 4<sup>th</sup> order DFT and Walsh function filters are identical. One observes in Figure 7 that the phase is continually changing, as well it should. However, the phase difference between to steady state single frequency signals should be constant which then allows impedance calculations based on (17). It is important to realize that Figures 4 through 7 are results for sampling a single frequency sine function, which is the ideal case.

$$Z_n = \frac{V_{RMS_n} \angle \Theta_{V_n}}{I_{RMS_n} \angle \Theta_{I_n}} = \frac{|V_{rms_n}|}{|I_{rms_n}|} \angle (\Theta_{V_n} - \Theta_{I_n}) \quad (17)$$



**Example of a Digital Time Overcurrent Relay Modeled in TACS**

An elementary algorithm to implement a time overcurrent relay is shown in equations in (18) through (20). Equation (18) provides the integrator algorithm with (19) and (20) the trip logic.



$$S_n = S_{n-1} + \left(\frac{I_{RMS_n}}{I_p} - 1\right)^a, S_n \geq 0 \quad (18)$$

$$IF(S_n \geq (T_0 + TDS \cdot T1)) \text{ then } Trip = True \quad (19)$$

$$\begin{aligned} &IF((TRIP == True) \text{ and } (S_n > 0)) \\ &\text{ then } TRIP = True \\ &\text{ else } TRIP = False \quad (20) \end{aligned}$$

The constant,  $I_p$ , in (18) is the minimum relay pickup current and  $\alpha$  provides inverse characteristics. If  $I_{RMSn}$  is less than  $I_p$ , then output of the integration decreases with a zero minimum limit. The logic expression in (19) provides the trip output while (20) keeps the trip output True until the integrator winds down to zero.  $T_0$  and  $T_1$  are time constants associated with the relay dynamics, while  $TDS$  is the time dial setting control.

Figure 8 provides a organization picture for what must be done mathematically to model a discrete time relay using TACS in EMTP. To operate closed-loop, the network section of EMTP must generate data for processing by TACS as well and accept outputs from TACS which can control the network structure by opening or closing switches. Not all the of processing blocks, {2} through {8}, will be implemented in this example although all may be required for authentic simulations. Equations (13) through (16) are used in block {5} based on Walsh functions. Block {4} forms the delayed samples needed for equations (13) and (14). The delayed samples are formed using the transport delay function in TACS. Equation (18) used in block {6}, and equations (19) and (20) in block {7}. Block {1} contains the network system data, which in this case is for the small system shown in Figure 9. Block {9} uses TACS controlled switches in the network.

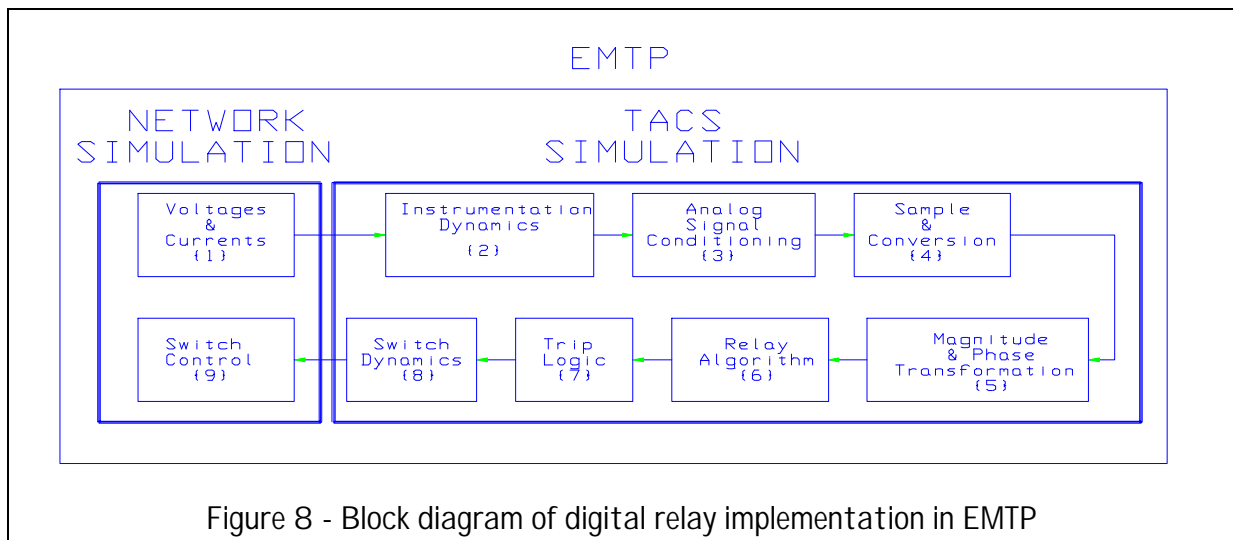
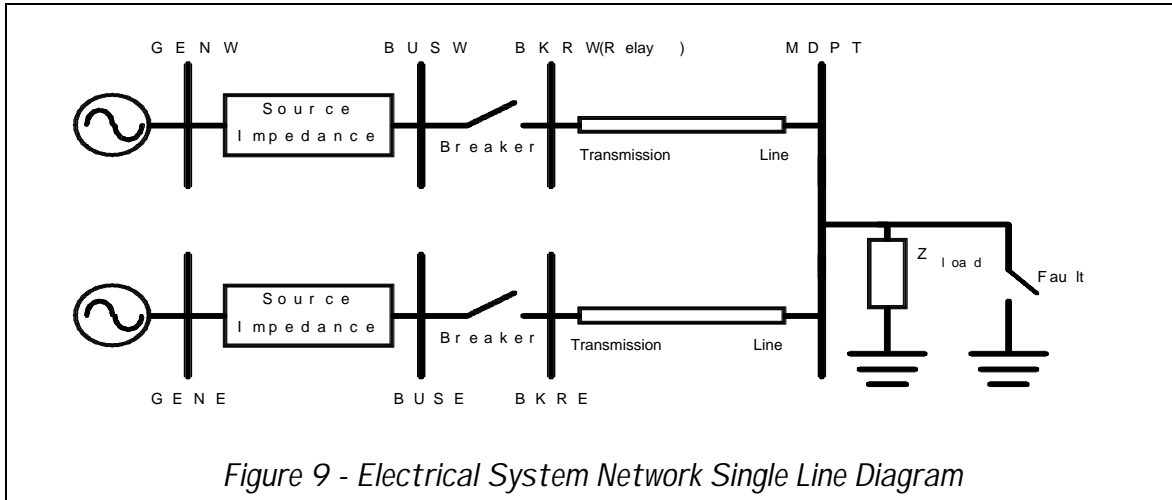


Figure 8 - Block diagram of digital relay implementation in EMTP

A digital non-directional time overcurrent relay simulation will detect the single line to ground fault that is applied at the load bus as also shown in Figure 9. Function blocks {2}, {3}, and {8} will not be implemented in this example. The digital time overcurrent relay model includes a reset time before reclosing. The sample digital relay model presented in this discussion is not intended to



represent the digital relays of any specific manufacturer.

Figure 10 shows the step change in AC current due to the fault switch being closed at 100 ms. The figure shows the instantaneous and RMS current measurements. The magnitude detector output has an initial transient because the Walsh function filter uses zero initial conditions. One can observe the Walsh function filter transient response to the fault as well as to the breaker opening and reclosing. Note also the magnitude detector is arbitrarily scaled for RMS output. It has been shown that this algorithm is high insensitive to DC offsets that are apparent in the figure.

Figure 11 shows the dynamics of various relay parameters. One can easily observe the transient response to the magnitude detector and see that the filter reacts to the transient caused by the closing of the fault switch by a slight over-shoot. If the magnitude of the fault current changed before the trip signal, one would observe a change in the slope of the integrator further reflecting the dynamics. This may be observed in the slight change in negative slope after the breaker opens. Figure 12 shows the TACS code for the relay implementation. The complete datafile for this case is shown in the Appendix.

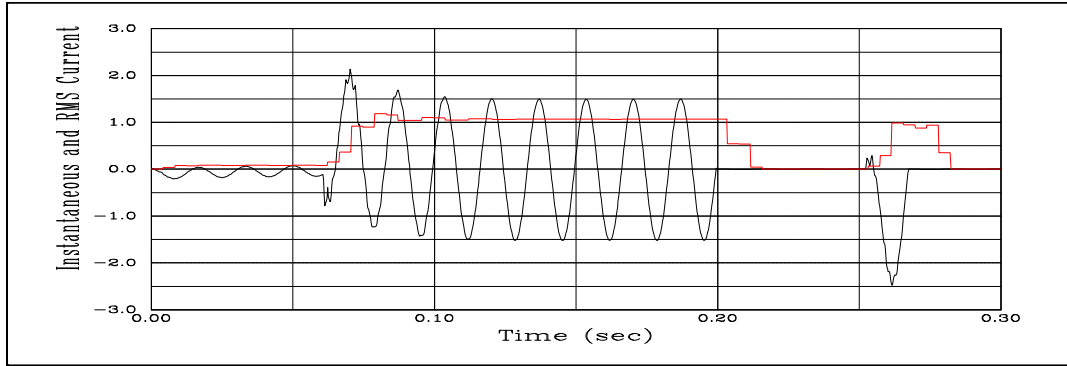


Figure 10 - Instantaneous and RMS current.

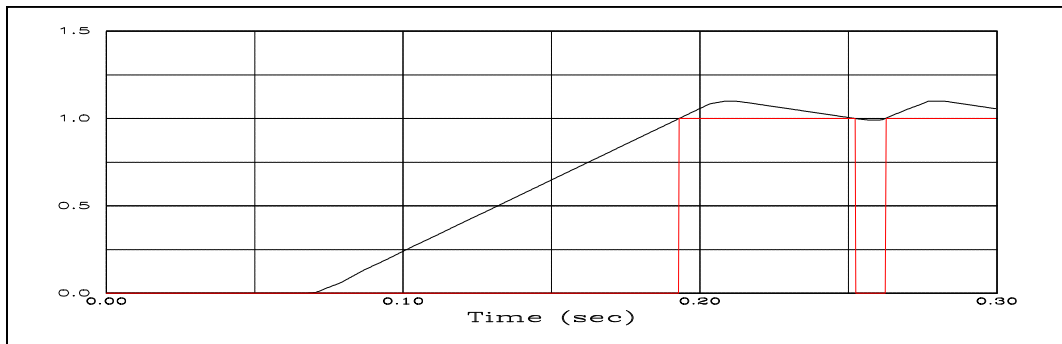


Figure 11 - Integrator Output and Trip Command to Switches

```

C ..... Time overcurrent relay .....
C Restraint spring constant
88WZLIM  =PLUS1/4
C
C First order integrator
C OUTPUT +IN1--> +IN2--> +IN3--> +IN4--> +IN5--> <-gain<--low<-highLOW-->HIGH-
>1WZINT  +WZRMS  -WZLIM                10.   0.  1.10
      1.
      0.      1.
C ..... Compute trip signal and grid fire control signal for EMTP .....
88WZTRP  =WZINT.GT.1.0
88WZGRD  =1.0-WZTRP
C
C ..... Initialize selected variables .....
C OUTPUT <-----A---
77WZGRD      1.
C
    
```

Figure 12 - TACS Implementation of Relay

### ***Conclusion***

An implementation strategy was presented for modeling digital relays in TACS with an interface to network in EMTP. The issues of breaker simulation in the EMTP network solution were addressed by using the TACS controlled switch type 11. The strategy included aspects of digital relaying concerned with processing sampled data such as instrumentation dynamics, signal conditioning for anti-aliasing, sample and hold, and breaker dynamics. A simple example of a non-directional time overcurrent was presented. Outputs from EMTP are shown to illustrate the kind of analysis possible with the approach presented in this paper.

### ***References***

- [1] A.V. Oppenheim and R.W. Schaffer, *Digital Signal Processing*. Prentice-Hall, Inc. Englewood Cliffs, NJ, 1985.
- [2] E.O. Schweitzer and A.J. Flechsig, "An Efficient Directional Distance Algorithm for Digital Computer Relaying", IEEE Conference Paper A 77 725-5, IEEE/PES Summer Meeting, Mexico City, Mexico, July, 1977.
- [3] A.J. Uranteta, R. Nadira, and L.G. Perez, "Optimal Coordination of Directional Overcurrent Relays in Interconnected Power Systems", *IEEE Transactions on Power Delivery*. Vol. 3, No. 3, July 1988, pp. 903-911.
- [4] J.N. Peterson and R.W. Wall, "Interactive Relay Controlled Power System Modeling", *IEEE Transactions on Power Delivery*. Vol. 6, No. 1, January, 1991, pp. 96-102.

## Appendix

```

BEGIN NEW DATA CASE
C *****
C     SIMPLE NON-DIRECTIONAL TIME OVER-CURRENT RELAY
C     AT WEST BUS - PHASE A WITH EMTP CIRCUIT FEEDBACK.  THE
C     RELAY VARIABLES ARE COMPUTED TWO WAYS: 1. CONTINEOUS
C     SAMPLING AT THE DeltaT INTERVAL and 2. SAMPLE & HOLD MODELING
C     OF AN A to D CONVERTER AT 4 SAMPLES PER 60 Hz CYCLE.
C *****
C DeltaT<---TMax<---XOpt<---COpt<-Epsilon<-TolMat<-TStart
      8.3E-5 300.E-3
C --IOut<--IPlot<-IDoubl<-KSSOut<-MaxOut<---IPun<-MemSav<---ICat<-NEnerg<-IPrSup
      15      3      0      0      0      1
C
C :::::::::::::::::::::::::::::: TACS data ::::::::::::::::::::::
TACS HYBRID
C OUTPUT <-----A-----B-----C----- <-T-START<-T-STOP--
91BKRWA          60.
C
C Sample generator for 240ms sampling A to D converter
C Variable|Amplitude| Period |Time high
C OUTPUT <-----A-----B-----C----- <-T-START<-T-STOP--
23SAMPL          1.1   .00415   .00003
C
C Generate AD converter samples at 240 ms intervals
C OUTPUT <-----A-----B-----C----- <-T-START<-T-STOP--
88WADZ0 62+BKRWA          SAMPL
C
C //////////////////////////////////////
C           DIGITAL CALCULATIONS
C SAMPLE AND HOLD delayed samples
C OUTPUTvv+IN1--> +IN2--> +IN3--> +IN4--> +IN5--> <--A--<--B--<--C--<--D--<--E--
88WADZ1 53+WADZ0          .00415
88WADZ2 53+WADZ0          .00830
88WADZ3 53+WADZ0          .01245
C
C OUTPUT +IN1--> +IN2--> +IN3--> +IN4--> +IN5--> <-gain<--low<-highLOW-->HIGH->
C
C ..... WALSH FUNCTION CALCULATIONS .....
C OUTPUT +IN1--> +IN2--> +IN3--> +IN4--> +IN5--> <-gain<--low<-highLOW-->HIGH->
WZSAL +WADZ0 +WADZ1 -WADZ2 -WADZ3          1.
WZCAL +WADZ0 -WADZ1 -WADZ2 +WADZ3          1.
88WZPHS =ATAN(WZSAL/WZCAL)*3960/7
88WZRMS =SQRT(WZSAL*WZSAL+WZCAL*WZCAL)/4
C ..... Time overcurrent relay .....
C Restraint sprin constant
88WZLIM =PLUS1/4
C
C First order integrator
C OUTPUT +IN1--> +IN2--> +IN3--> +IN4--> +IN5--> <-gain<--low<-highLOW-->HIGH->
1WZINT +WZRMS -WZLIM          10.  0.  1.10

```

```

1.
0.      1.
C ..... Compute trip signal and grid fire control signal for EMTP .....
88WZTRP  =WZINT.GT.1.0
88WZGRD  =1.0-WZTRP
C
C ..... Initialize selected variables .....
C OUTPUT <-----A---
77WZGRD      1.
C
C #####
C #                OUTPUT FROM TACS                #
C ----->----->----->----->----->----->----->----->----->
33WZRMS WZPHS WAINW WATRP WZINT WZTRP WZGRD
BLANK End of TACS
C *****
C
C .....Circuit data.....
C %%%%%%%%%%
C %                Source Impedances                %
C Bus-->Bus--><-----><---R<-----L<---R<-----L<---R<-----L
51WESTA BUSWA      .13      23.71      0
52WESTB BUSWB      .06      39.99      0
53WESTC BUSWC
C %%%%%%%%%%
C Bus-->Bus--><-----><---R<-----L<---R<-----L<---R<-----L
51EASTA BUSEA      0        84.2      0
52EASTB BUSEB      0        154.4     0
53EASTC BUSEC
C %%%%%%%%%%
C %                Line WEST TO EAST                %
C %%%%%%%%%%
C Bus-->Bus-->Bus-->Bus--><---R'<---L'<---C'<---len 0 0 0<-----Blank----->0
-1TACWA MDPTA      0.3167 3.222.00787 193.1 0 0 0
-2BKRWB MDPTB      0.0243 .9238 .0126 193.1 0 0 0
-3BKRWC MDPTC
C %%%%%%%%%%
C %                Line EAST TO WEST                %
C %%%%%%%%%%
C Bus-->Bus-->Bus-->Bus--><---R'<---L'<---C'<---len 0 0 0<-----Blank----->0
-1BKREA MDPTA      0.3167 3.222.00787 144.4 0 0 0
-2BKREB MDPTB      0.0243 .9238 .0126 144.4 0 0 0
-3BKREC MDPTC
C %%%%%%%%%%
C %                Load at MDPT                    %
C %%%%%%%%%%
C Bus-->Bus-->Bus-->Bus--><---R'<---L'<---C'<---len 0 0 0<-----Blank----->0
MDPTA      251.2 219.1      0
MDPTB      251.2 219.1      0
MDPTC      251.2 219.1      0
C %%%%%%%%%%
C %                FAULT at MDPT                    %
%

```

```

C %%%%%%%%%%%%%%%%%%%%%%%%%%%%%%%%%%%%%%%%%%%%%%%%%%%%%%%%%%%%%%%%%%%%%%%%%
C Bus-->Bus-->Bus-->Bus--><---R'<---L'<---C'<---len 0 0 0<-----Blank----->O
MDPTA FSA                                1.0                                0
C %%%%%%%%%%%%%%%%%%%%%%%%%%%%%%%%%%%%%%%%%%%%%%%%%%%%%%%%%%%%%%%%%%%%%%%%%
C %                                TACS CONTROLLED SWITCH SEPERATOR                                %
C %                                (See TACS controlled switch below)                                %
C %%%%%%%%%%%%%%%%%%%%%%%%%%%%%%%%%%%%%%%%%%%%%%%%%%%%%%%%%%%%%%%%%%%%%%%%%
C Bus-->Bus-->Bus-->Bus--><---R'<---L'<---C'<---len 0 0 0<-----Blank----->O
TAC1A TACWA                              1.0E-3                              0
TAC1B TACWA                              1.0E-3                              0
C %%%%%%%%%%%%%%%%%%%%%%%%%%%%%%%%%%%%%%%%%%%%%%%%%%%%%%%%%%%%%%%%%%%%%%%%%
BLANK End of circuit data.....|
C
C .....Switch data.....
C Bus-->Bus--><---Tclose<---Topen<-----Ie                                O
BUSWA BKRWA                               -1.           9999           0                                1
BUSWB BKRWB                               -1.           9999           0                                1
BUSWC BKRWC                               -1.           9999           0                                1
C %%%%%%%%%%%%%%%%%%%%%%%%%%%%%%%%%%%%%%%%%%%%%%%%%%%%%%%%%%%%%%%%%%%%%%%%%
C Bus-->Bus--><---Tclose<---Topen<-----Ie                                O
BUSEA BKREA                               -1.           9999           0                                1
BUSEB BKREB                               -1.           9999           0                                1
BUSEC BKREC                               -1.           9999           0                                1
C %%%%%%%%%%%%%%%%%%%%%%%%%%%%%%%%%%%%%%%%%%%%%%%%%%%%%%%%%%%%%%%%%%%%%%%%%
C % ..... FAULT SWITCH ..... %
C Bus-->Bus--><---Tclose<---Topen<-----Ie                                O
FSA             60.00E-3           9999           0                                1
C %%%%%%%%%%%%%%%%%%%%%%%%%%%%%%%%%%%%%%%%%%%%%%%%%%%%%%%%%%%%%%%%%%%%%%%%%
C % ..... TACS CONTROLLED SWITCH ..... %
C % The SCR switch model so switch opens at current zero crossing. %
C % TACS does not allow type 11 switches to operate in parallel without a %
C % series impedance to sepearate the switches. (See TAC1A and TAC1B above.) %
C Bus-->Bus--><---Vig---<---Iholh---<---tdeion---<////////<Close< " <---GRID<Open < OO
11BKRWA TAC1A           0.           0.           0.                                WZGRD           1
11TAC1B BKRWA           0.           0.           0.                                WZGRD           1
BLANK End of switch data.....|
C
C .....Source data.....
C %%%%%%%%%%%%%%%%%%%%%%%%%%%%%%%%%%%%%%%%%%%%%%%%%%%%%%%%%%%%%%%%%%%%%%%%%
C % Peak Line to Ground Voltage for 230 kV RMS Voltage Source is 187.79 kV %
C % Normalized with Vbase = 1 kV %
C %%%%%%%%%%%%%%%%%%%%%%%%%%%%%%%%%%%%%%%%%%%%%%%%%%%%%%%%%%%%%%%%%%%%%%%%%
C Bus--><I<Amplitude<Frequency<---T0|Phi0<---0=Phi0           <---Tstart<---Tstop
14WESTA           187.79           60.           0.           0.                                -1.           9999.
14WESTB           187.79           60.          -120.           0.                                -1.           9999.
14WESTC           187.79           60.           120.           0.                                -1.           9999.
14EASTA           187.79           60.           15.           0.                                -1.           9999.
14EASTB           187.79           60.          -105.           0.                                -1.           9999.
14EASTC           187.79           60.           135.           0.                                -1.           9999.
BLANK End of source data.....|
C
C
C

```

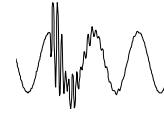
```
C
C .....Output Request Data.....
C Bus-->Bus-->Bus-->Bus-->Bus-->Bus-->Bus-->Bus-->Bus-->Bus-->Bus-->
  BKRWA BKRWB BKRWC BKREA BKREB BKREC MDPTA MDPTB MDPTC
BLANK End of output requests.....|
BLANK End of Plot Request.....|
BLANK End of All Cases
```

*Richard W. Wall, University of Idaho  
Brian K. Johnson, University of Idaho*

*BLANK PAGE*

# ***Voltage Notching Concerns***

---



## ***Voltage Notching Concerns Associated with a Large Induction Motor Dive***

### ***Introduction***

Adjustable speed drives are used with very large synchronous and induction motors (e.g. 1-20,000 hp) for a variety of reasons. The drives can result in significantly improved efficiency when the driven load is variable. For large motor applications on weak systems, the drives may be required for motor starting to avoid high inrush currents.

For large motors, drives typically use phase-controlled rectifiers (SCRs) and a large dc link inductor to supply a relatively constant dc current to the inverter. This is known as a current source inverter (CSI) configuration. The input rectifier may be configured as a six pulse or twelve pulse rectifier, depending on harmonic control requirements.

The voltage notching discussed in this paper is caused by the commutating action of the controlled rectifier. Whenever the current is commutated from one phase to another, there is a momentary phase-to-phase short circuit through the rectifier switching devices (SCRs, in this case). For a six pulse converter, this happens six times each cycle. The voltage notch is defined by its duration and its depth. The duration (known as the commutation period) is determined by the source inductance to the drive and the current magnitude. The depth of the notch is reduced by inductance between the observation point and the drive (e.g. isolation transformer or choke inductance). An example waveform illustrating simple notches resulting from a drive operation is shown in Figure 1.

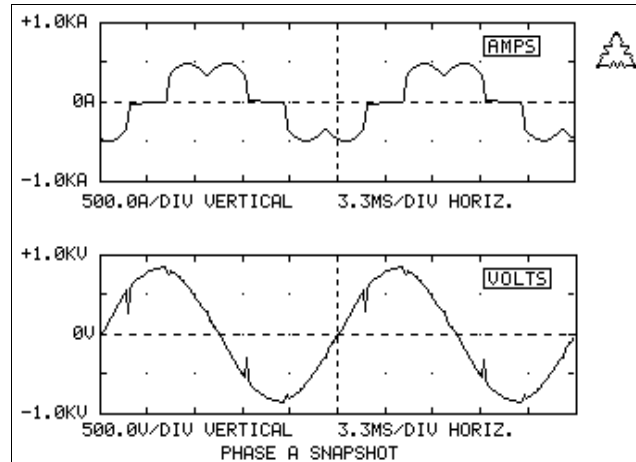


Figure 1 - Example of voltage notches caused by converter commutation.

On most systems, problems with voltage notching can be minimized by applying sufficient isolation reactance. This limits the notch magnitude on the source side of the isolation reactance. However, on some systems, the notches that appear at the system level can still be significant. If there is not much resistive load on a system like this, the notches can excite the natural frequency of the distribution system (determined by the capacitance of lines, cables, and capacitor banks in parallel with the system source inductance) and cause significant distortion in the voltage waveform.

## Description of Example System

The analysis in this paper focuses on a particular example system where the voltage notching caused significant oscillations at the distribution system level, resulting in equipment problems at another customer supplied from the same system. The example system is illustrated by the one line diagram in Figure 2.

The 25 kV distribution system is supplied through a 10 MVA transformer from the 144 kV transmission system. The customer causing the notching problems has a 6000 hp induction motor supplied through an adjustable speed drive. This drive is at a 4.16 kV bus supplied through a 7.5 MVA transformer. Harmonic filters (5th, 7th, 11th) are included to control the lower order characteristic harmonics of the six pulse drive.

Another customer on a parallel feeder supplied from the same 25 kV bus has motor loads at both 4.16 kV (800 hp motor) and 480 volts. The 800 hp motor includes surge capacitors for transient protection. The customer also has power factor correction capacitors at the 480 volt bus. These lower voltage

surge capacitors and power factor correction capacitors have the potential to magnify the oscillations which occur on the distribution system.

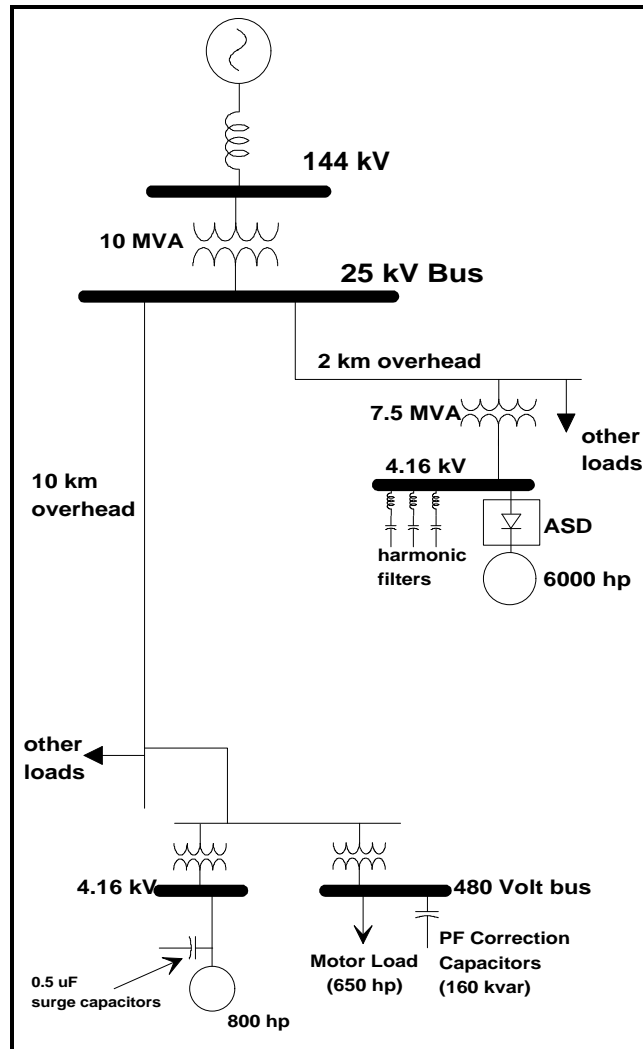


Figure 2 - One line diagram for example system.

### Problem Description

Operation of the 6000 hp motor and drive resulted in significant oscillations on the 25 kV supply system. These oscillations caused clocks to run fast at the customer with the 6000 hp motor and failure of surge capacitors on the 800 hp motor at the customer located on the parallel feeder.

Figure 3 illustrates the measured waveforms on the 25 kV supply system. The oscillations have a primary frequency component near the 60th harmonic. In

this case, the natural frequency is the result of the line capacitance from approximately 12 km of overhead line in parallel with the system source inductance. Note that the oscillations are excited six times per cycle corresponding to the six-pulse operation of the drive.

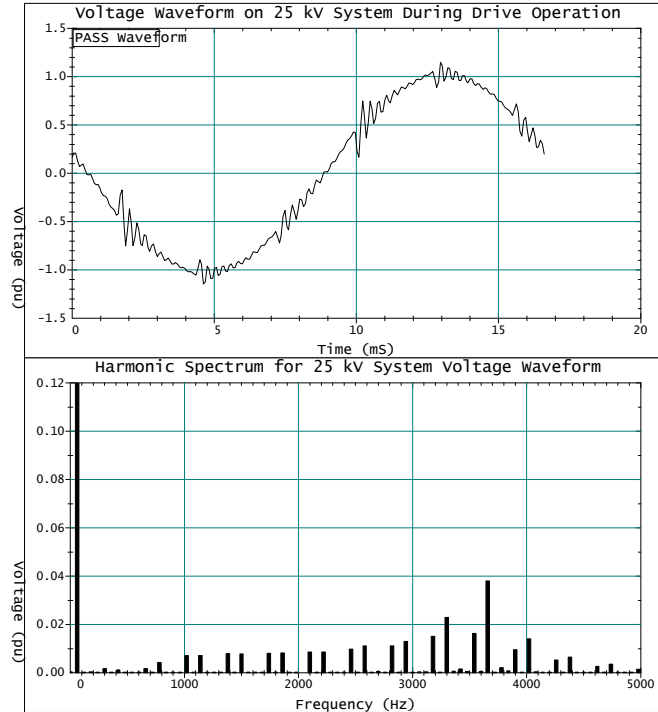


Figure 3 - Voltage waveform and spectrum on 25 kV system during drive operation.

### ***Analysis of the Problem***

A model was developed using the electro-magnetic transients program (EMTP) to evaluate the magnification at the surge capacitor location and to evaluate possible solutions to the problem. First of all, the steady state frequency response of the system was simulated to illustrate the natural frequency that can excite the oscillations illustrated above. Figure 4 shows the voltage on the 25 kV system as a function of a 1 amp source at the 4.16 kV bus where the drive is located. The system resonance just above the 60th harmonic is apparent in the figure.

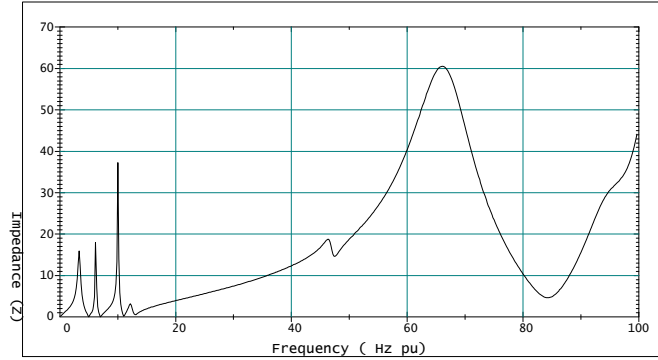


Figure 4 - Voltage vs. frequency at 25 kV bus due to 1 amp source at 4.16 kV drive location

Next, the actual adjustable speed drive and motor load were represented to reproduce the notching oscillations observed in the measurements. The worst notching problems are associated with a firing angle at about 70% load. The simulated waveform for the 25 kV bus voltage is shown in Figure 5 below. The oscillations at each commutation point are in good agreement with the measurement results.

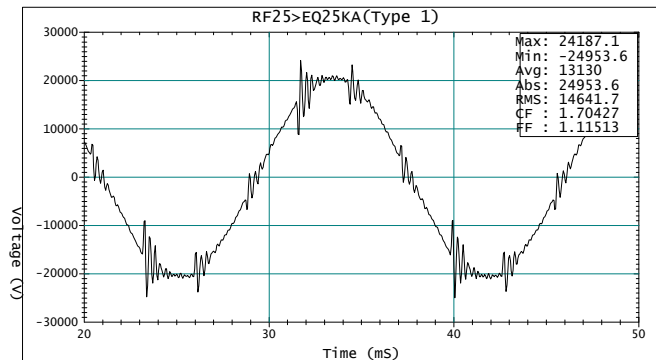


Figure 5 - Simulated 25 kV system voltage with drive operating.

The model was then used to evaluate the voltage waveforms at the customer bus located on the parallel feeder. Figure 6 illustrates the voltage waveform at the 4.16 kV bus where the 800 hp motor surge capacitors cause magnification of the oscillations. The potential for problems at this location is quite evident. The surge capacitors fail because this voltage is imposed on them continuously, resulting in overheating and failure.

Figure 7 shows the waveform at the 480 volt bus where the power factor correction capacitors damp out the high frequency oscillation. The power factor correction capacitors are much larger than the surge capacitors and result in a

much lower resonant frequency. No problems were encountered with loads on the 480 volt bus.

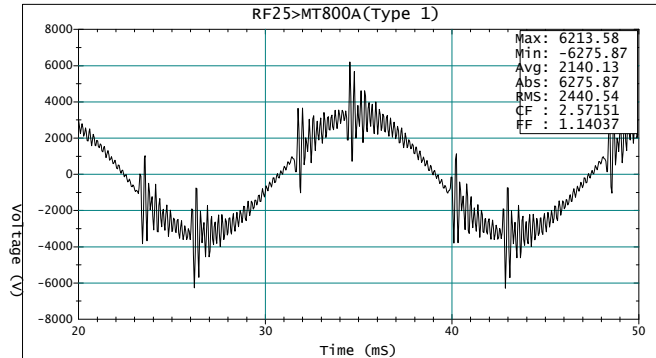


Figure 6 - Simulated waveform at surge capacitor location (4.16 kV bus of customer on parallel feeder).

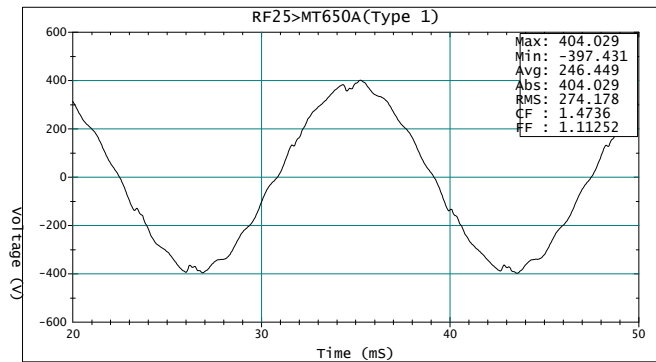


Figure 7 - Simulated waveform at power factor correction capacitors (480 volt bus of customer on parallel feeder).

## Possible Solutions to the Problem

A number of possible solutions to the high frequency oscillation problem were evaluated. These included:

1. A larger choke inductance at the input to the adjustable speed drive. This approach could be effective if the choke impedance was included as part of the drive's initial design. As a retrofit, it is impractical because the size required would cause voltage regulation problems at the drive.
2. Larger surge capacitors at the 800 hp motor of the parallel customer. This approach is feasible to protect the individual motor and surge capacitors of concern. However, large surge capacitors would be required and they do not eliminate the oscillations on the 25 kV system that are

- the source of the problem. If the oscillations on the 25 kV system are not reduced, other customers could experience similar problems.
3. Modification of the filtering at the adjustable speed drive to include a high pass filter instead of just tuned branches at the 5th, 7th, and 11th. This approach proved to be ineffective because the high pass filter cannot provide sufficient damping at the higher frequency resonance.
  4. Addition of a capacitor bank on the 25 kV system. This approach has the advantage of being the most practical to implement. Simulations show that this solution can be effective.

### ***Sizing the Capacitor Bank***

The solution of adding a capacitor bank on the 25 kV system was evaluated in the most detail. The concern for this approach is that added capacitors will result in a system resonance that could excite one of the lower order characteristic harmonics of the drives.

Since the drive includes harmonic filters at the 5th, 7th, and 11th harmonics, it should be possible to add a capacitor to the 25 kV system that moves the system resonance to somewhere between the 7th and 11th harmonics without causing a problem. A 1200 kvar capacitor bank was tried first but this created a resonance that magnified the thirteenth harmonic component on the system if the power factor correction capacitors at the parallel customer were out of service. Figure 8 gives the measured voltage on the 25 kV system for this condition. Note that the notching oscillation problem is solved but the thirteenth harmonic component in the voltage is approaching 5%.

After examination of the system frequency response with the drive filters and the existing load power factor correction capacitors, the capacitor size was increased to 2400 kvar to solve the thirteenth harmonic resonance problem. Figure 9 illustrates the frequency response at the 25 kV bus for a 1 amp source located at the 4.16 kV drive location. All of the system resonances that cause magnification are located below the eleventh harmonic and are at frequencies that are not characteristic harmonics of the drive. Figure 10 gives the measured voltage waveform and harmonic spectrum with the 2400 kvar capacitor operational. The voltage distortion is less than 2% with the 2400 kvar capacitor in service.

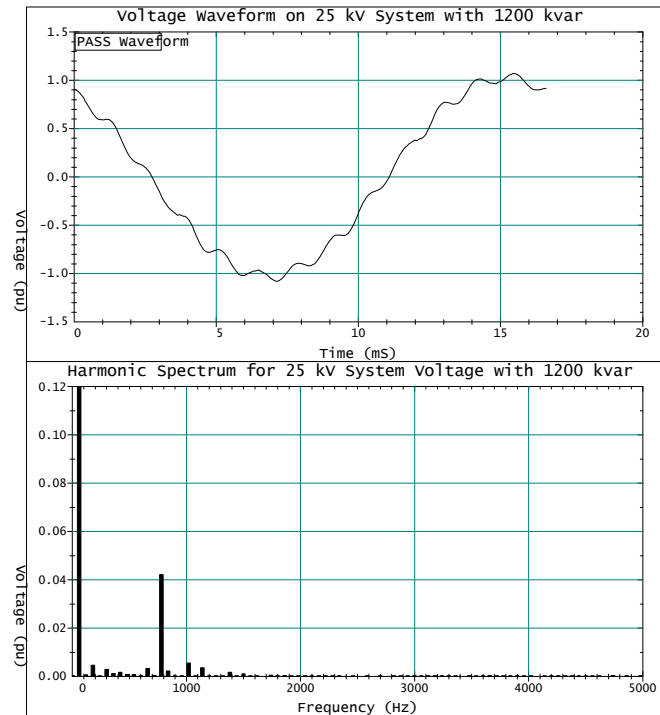


Figure 8 - Voltage waveform and spectrum on 25 kV system with a 1200 kvar capacitor bank in service and the customer power factor correction capacitors off.

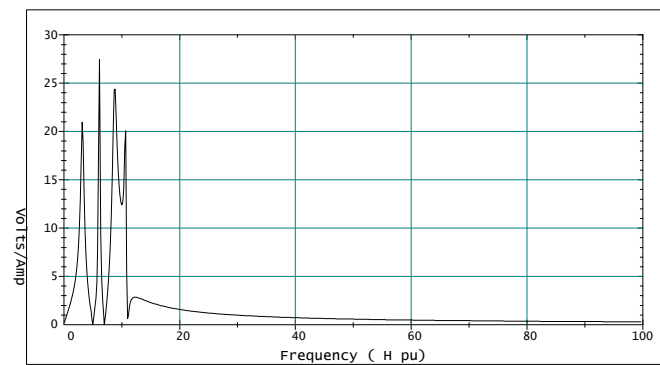


Figure 9 - Voltage vs. frequency at 25 kV bus due to a 1 amp source at the 4.16 kV drive location with 2400 kvar capacitor in service at the 25 kV bus.

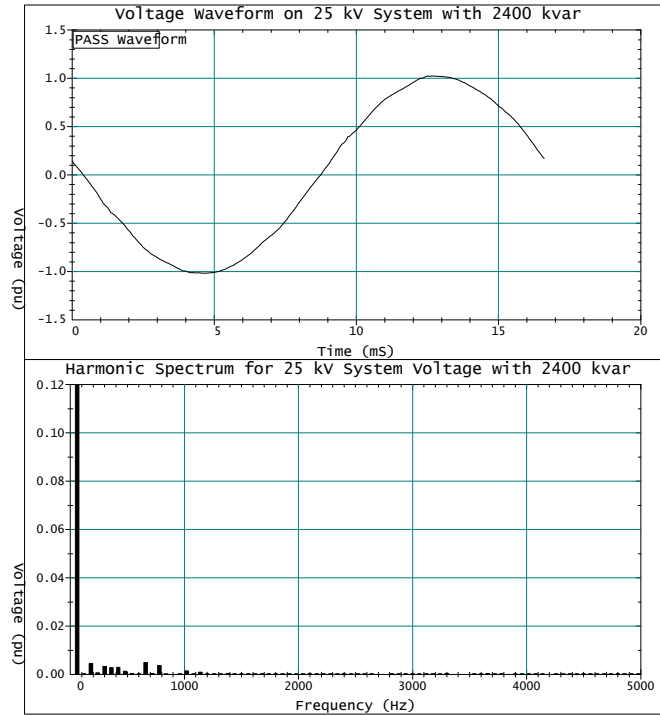


Figure 10 - Voltage waveform and spectrum on 25 kV system with a 2400 kvar capacitor bank in service.

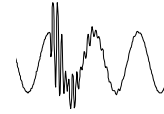
## Conclusions

- This paper illustrates the characteristics of system oscillations that can result from the notching of a large adjustable speed drive operating on a relatively low short circuit level supply system without significant resistive load for damping.
- The system oscillations can be magnified at customer locations where low voltage capacitors exist. Small capacitors, such as motor surge capacitors can be a particular problem.
- This problem can be solved by careful selection of a capacitor size for the primary distribution system. The capacitor should not introduce a new resonance at one of the characteristic harmonics of the adjustable speed drive. The interaction of the proposed capacitor with other system capacitors and harmonic filters must be evaluated.

Len Hawreliak, Sharon Morganson, Alberta Power  
 Ralph Ferraro, Ferraro, Oliver & Associates  
 Le Tang, Erich Gunther, Mark McGranaghan, Electrotek Concepts, Inc.

**BLANK PAGE**

# Module Development Follow-up



## EMTP Data Modules - Include File Structure

The development of EMTP data modules was previously discussed in the EMTP Tech Notes Issue 93-1 and again in the workbook for the 1994 EMTP Case Study Workshop - "EMTP Data Modules". As a follow-up to those references, I would like to discuss the information presented in the "include" files (typically \*.INC or \*.PCH).

In addition, I would like to illustrate a conversion bug that was found after the workshop presentation.

The process of developing an EMTP data module includes converting the data module (\*.MOD) into an include file (using MODULE command in the EPRI/DCG version and the DATA BASE MODULE command in ATP). The resulting include file has a header similar to Table 1.

Table 1 - Example EMTP Data Module Include File Header

KARD	2	2	2	3	3	3	4	4	4
KARG	1	2	3	1	2	3	1	2	3
KBEG	3	39	80	3	39	80	3	39	80
KEND	7	44	80	7	44	80	7	44	80
KTEX	1	0	1	1	0	1	1	0	1

The header includes information regarding:

- Number of substitutions in the module
- Number of arguments in the module
- Number of dummy variables in the module
- The cards (rows) and columns where arguments and dummy variables have to be replaced
- The mode of variable substitution (alphanumeric or numeric).

The first line of the header "KARD" refers to the number of the non-commented card, where the argument given by "KARG" has to be replaced. The parameter KARG refers to the number of the argument, with negative numbers illustrating dummy variables.





Another example - referring to the second column in the header,

KARD	2
KARG	2
KBEG	39
KEND	44
KTEX	0

yields the following information

On card 2 (KARD 2), there is the second (KARG = 2) numeric (KTEX = 1) variable that begins in column 39 (KBEG = 39) and ends in column 44 (KEND = 44). This variable (CPHASE) is shown in bold italic type for clarity.

This process continues until all of the substitutions in the include file have been defined.

### ***EMTP Data Modules - Include File Bug***

Soon after the last EMTP Case Study Workshop - EMTP Data Modules (September, 1994), one of the members of the User's Group (Jeff Peggs of Virginia Power) attempted to modify one of the module files that had been distributed at the meeting. The module was for a three-phase equivalent (3PHEQUIV). Two of the parameters were the start-time and stop-time for the Type 14 voltage source. When Jeff attempted to "hardcode" the start and stop times to -1.0E-03 and 9999.9 respectively, he found that the module would no longer work when called from the EMTP data case. Jeff assumed that there was a problem with the module, so he asked me to look into the changes to see what could be causing the error.

After a number of attempts on my part (actually a rather large number), I found that the include file header had a row that looked similar to:

KARD	2	2	2	3	3	3	4	4	4
	0								
...									
...									
...									
etc									





Table 6 - Module File for Corrected BUGWYEG

```

C EMTP Data Module: BUGWYEG
C
C Description: Three-Phase Grounded-Wye RLC Simple RLC Bank
C
C Created: 10/27/94 (TEG/LT) Last Updated: 10/27/94 (TEG)
C
C Usage: BUGWYEG KNODE, RPHASE, LPHASE, CPHASE, ?, @
C
ARG KNODE, RPHASE, LPHASE, CPHASE, ?, @          ; ARGUMENTS
C
NUM          RPHASE, LPHASE, CPHASE              ; NUMERIC PARAMETERS
C
/BRANCH
C <---Nodes--><---Refer--><-Ohms<---mH<---uF<-----Out
C Bus1->Bus2->Bus3->Bus4-><---R<---L<---C          V
  KNODEA          RPHASELPHASECPHASE            1
  KNODEB          RPHASELPHASECPHASE            @
  KNODEC          RPHASELPHASECPHASE            @
C .....^.....^.....^.....^.....^.....^.....^.....^xxxxxxxxxxxxxxxxxxxxxxxxxxxxxxxxxxxxxxxx^
C
/ENDMODULE
$EOF

```

Table 7 - Include File for Corrected BUGWYEG

KARD	2	2	2	2	3	3	3	3	3	4	4	4	4	4
KARG	1	2	3	4	1	2	3	4	6	1	2	3	4	6
KBEG	3	27	33	39	3	27	33	39	80	3	27	33	39	80
KEND	7	32	38	44	7	32	38	44	80	7	32	38	44	80
KTEX	1	0	0	0	1	0	0	0	1	1	0	0	0	1

```

C EMTP Data Module: BUGWYEG
C
C Description: Three-Phase Grounded-Wye RLC Simple RLC Bank
C
C Created: 10/27/94 (TEG/LT) Last Updated: 10/27/94 (TEG)
C
C Usage: BUGWYEG KNODE, RPHASE, LPHASE, CPHASE, ?, @
C
C
C
/BRANCH
C <---Nodes--><---Refer--><-Ohms<---mH<---uF<-----Out
C Bus1->Bus2->Bus3->Bus4-><---R<---L<---C          V
  KNODEA          RPHASELPHASECPHASE            1
  KNODEB          RPHASELPHASECPHASE            @
  KNODEC          RPHASELPHASECPHASE            @
C .....^.....^.....^.....^.....^.....^.....^.....^xxxxxxxxxxxxxxxxxxxxxxxxxxxxxxxxxxxxxxxx^
C

```

```
/ENDMODULE
$EOF
$EOF **** END OF FILE ****
DATE AND TIME OF MODULE CONVERSION:    10/27/94  16.44.03
NUMBER OF ARGUMENTS DECLARED IN THIS MODULE:    6
NUMBER OF DUMMY VARIABLES DECLARED IN THIS MODULE:    0
                **USER-SUPPLIED HEADER CARDS FOLLOW**
ARG KNODE, RPHASE, LPHASE, CPHASE, ?, @          ; ARGUMENTS
NUM          RPHASE, LPHASE, CPHASE              ; NUMERIC PARAMETERS
; NUMERIC PARAMETERS
```

This problem will be passed along to program developers so it can be corrected in subsequent versions. However, in the interim, the work-around just described should allow users to continue to use modules.

*Tom Grebe, Le Tang - Electrotek  
Jeff Peggs - Virginia Power*